# Self-Normalization of 3D PET Data by Estimating Scan-Dependent Effective Crystal Efficiencies

Martin A. Belzunce and Andrew J. Reader

***Abstract*—Normalization of the lines of response (LORs) or sinogram bins is necessary to avoid artifacts in fully 3D PET imaging. Component-based normalization (CBN) is an effective strategy to generate normalization factors (NFs) from short time scans of known emission sources. In the CBN, the NFs can be factorized into time-invariant and time-variant components. The effective crystal efficiencies are the main time-variant component, and a frequent normalization scan is needed to update their values. Therefore, it would be advantageous to be able to estimate unique effective crystal efficiencies to account for this time-variant component. In this work, we present a self-normalization algorithm to estimate the crystal efficiencies directly from any emission acquisition. The algorithm is based on the principle that if the true image were known, the mismatch between its projections, corrected for the time-invariant NFs, and the acquired data could be used to estimate the effective crystal efficiencies. We show that the algorithm successfully estimates the effective crystal efficiencies for simulated sinograms with different levels of Poisson noise and for different distributions of crystals efficiencies. This algorithm permits the reconstruction of good quality images without the need for an independent, separate, normalization scan. A key advantage of the method is the estimation of relatively few parameters ($\sim 10^4$) compared to the number of NFs for 3D data ($\sim 10^8$).**

## I. Introduction

In positron emission tomography (PET), each line of response (LOR) has a different sensitivity due to the scanner's geometry and the detector properties, such as the detection profile of a block detector or the variations in the crystal efficiencies. In order to achieve artifact-free and good quality images, these non-uniformities must be modelled using normalization factors (NFs) or precorrected using normalization correction factors (NCFs). A widely used normalization method is the component-based normalization (CBN), where the number of parameters to estimate is dramatically reduced by modelling the efficiency of each LOR as a product of multiple factors [1].

In the CBN, the components can be separated into time-invariant (e.g. geometry and block profile), time-variant (effective crystal efficiencies) and acquisition-dependent (dead-time) components. The time-variant factors are updated by a regular normalization scan. The effective crystal efficiencies can change between normalization scans for many reasons, including, for example, variations in temperature. Therefore, it would be advantageous to be able to estimate the effective crystal efficiencies directly for each unique emission scan.

In this work, we present a self-normalization algorithm to estimate the effective crystal efficiencies directly from the emission data. Other approaches to self-normalization have been presented before to obtain the NFs from coincidences [2] or singles [3] data, and also to correct for pile-up in block detectors [4]. In our method, we focus on a self-normalization that takes advantage of the time-invariant correction factors and, as a consequence, the number of parameters to estimate is reduced by a factor of $10^4$, as only the effective crystal efficiencies are needed. The self-normalization algorithm was evaluated using simulated data with four different distributions of crystal efficiencies.

Martin A. Belzunce and Andrew J. Reader are with King's College London, Division of Imaging Sciences and Biomedical Engineering, St Thomas Hospital, London, UK.

## II. Materials and Methods

We applied our method to the normalization scheme used by the Biograph mMR, a simultaneous PET-MR scanner [5], which uses a component-based normalization that models the geometry, the crystal interference in the block detectors, the crystal efficiencies, the dead-time and the axial profile [6] of the scanner. We classified the factors as time-invariant, time-variant and acquisition-dependent:

$$N_C = N_{TI} \cdot N_{TV} \cdot N_{AQ} \tag{1}$$

where $N_C$ are the complete normalization factors, $N_{TI}$ are the time-invariant, $N_{TV}$ are the time-variant and $N_{AQ}$ are the acquisition dependent NFs. In this work, we focus on $N_{TI}$ and $N_{TV}$, hence we use $N_{AQ} = 1$. These NFs are stored in a diagonal matrix with as many rows and columns as the total number of bins in the sinogram.

### A. Self-Normalization Algorithm

A reconstructed image without the correct normalization generates artifacts and a mismatch from the true emission distribution. If the true image were known, the mismatch between its projections (when divided by $N_{TI}$) and the acquired data can be used to estimate the crystal efficiencies. Based on this principle, we designed an algorithm to estimate the effective crystal efficiencies directly from the emission data.

The algorithm needs an operator to map from NF sinograms to crystal efficiencies. We designed an operator based on the fan-sum algorithm [7], [8]. We define this operator using two matrices $D_1$ and $D_2$ that identify each of the two crystal elements associated with a given sinogram bin. The operator, hereinafter referred to as $C[]$, uses a combination of both matrices to reduce the statistical uncertainty for those crystals that are partially present in each matrix:

$$x = C[n_{TV}] = \frac{D_1^T n_{TV} + D_2^T n_{TV}}{D_1^T 1 + D_2^T 1} \tag{2}$$

where $D_1$ is the matrix for group 1 of the crystal elements, that has as many rows as bins in the sinogram and as many columns as there are crystal elements; $D_2$ is an equivalent matrix for the second group of crystals in the sinogram. $n_{TV}$ is a column vector with the bins of the time-variant normalization sinogram and 1 is a unit-valued column vector of the same size of $n_{TV}$. The result of $C[n_{TV}]$ is the vector $x$ with the effective crystal efficiencies. The diagonal matrix

$N_{TV}$ used in the forward model for EM reconstruction is obtained from the vector $n_{TV}$ by:

$$N_{TV} = diag(n_{TV}) \tag{3}$$

We used the operator $C[]$ to design a self-normalization algorithm that estimates the crystal efficiencies for each emission scan. It starts with unit crystal efficiencies ($x^0$) and has six steps, that must be repeated at least twice to arrive at the solution. The steps in each iteration are:

1) The time-variant NFs ($N^k_{TV}$) are generated from the current crystal efficiencies estimate $x^k$.
2) The complete NFs are generated with $N^k_C = N^k_{TV} \cdot N_{TI}$.
3) The measured emission fully 3D sinogram data $b$ is reconstructed into image $f^k$ with an OP-OSEM algorithm using $N^k_C$ as the NFs.
4) $f^k$ is projected into a sinogram $p^k$ and the complete forward model is applied.
5) $C[]$ is applied to the projected ($p^k$) and to the input ($b$) sinograms.
6) The ratio between $C[b]$ and $C[p^k \circ N^k_C + r + s]$ is computed and then normalized to get a multiplicative correction factor for the current crystal efficiencies.

The whole process is summarized with the following equation:

$$x^{k+1} = x^k \cdot \frac{C[b]}{C[N^k_{TV} \circ N_{TI} \circ A f^k + r + s]} \tag{4}$$

where $x^k$ is the current estimate of the crystal efficiencies, $C[]$ is the operator defined in (2), $\circ$ is the element by elment multiplication, $b$ is the emission sinogram, $N^k_{TV}$ are the time-variant NFs in iteration k, $N_{TI}$ are the time-invariant NFs, $A$ is the geometric system matrix and $f^k$ is the current reconstructed image. $r$ and $s$ are the randoms and scatter estimates, but they were not used in this work since we did not simulate these effects.

The $N^k_{TV}$ matrix is obtained in each iteration by applying the equation (5) and storing the result in a diagonal matrix:

$$n^k_{TV} = D_1 x^k \circ D_2 x^k \tag{5}$$

Finally, is important to clarify that we perform the ratio in crystal space instead of sinogram space, because this was an effective way to reduce the number of elements used in the correction ratio; and as a result improve the stability and robustness of the algorithm.

### *B. Algorithm Evaluation*

To evaluate the self-normalization algorithm, we simulated 4 different sets of crystal efficiencies. The first set contains the crystal efficiencies of a Siemens mMR normalization file (set 1). Then, we created crystal efficiencies with a normal distribution with mean 1 and a standard deviation of 5 and 10 times that of set 1 (referred to here as set 2 and 3 respectively). Finally, as an extreme case, we simulated a set with a uniform distribution between 0 and 2 (set 4).

For each set of crystal efficiencies, we simulated 3D sinograms by projecting a uniform cylinder in one case, and a brain phantom [9] in a second case, and multiplying them by the complete NFs ($N_C$). We created noise-free sinograms, as well as with Poisson noise. The latter were produced by scaling the noise-free sinograms to get mean values ($\lambda$) of 1 to 100 counts in the sinogram and, then, generating a Poisson random number of counts for each bin. We used the geometry and sinogram dimensions (span 1) corresponding to the Biograph mMR, where each bin of the sinogram corresponds to an LOR between a unique pair of crystals and there are zero-valued bins for the gaps between the block detectors.

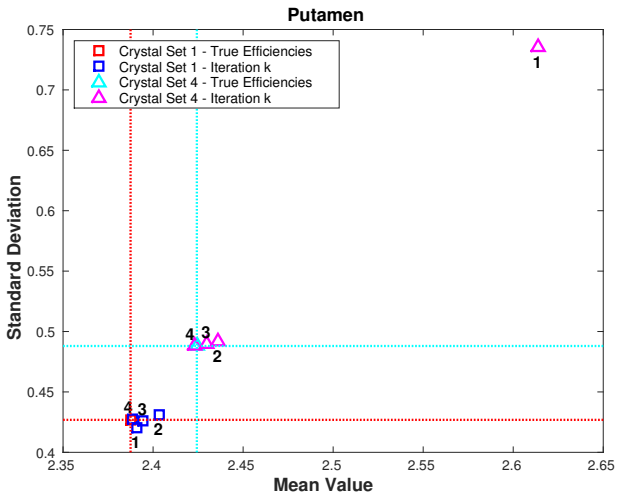


Fig. 1. SD and mean values in the putamen for each iteration of the self-normalization algorithm for the reconstruction of noisy sinograms ($\lambda = 10$). Each pair of values is labelled with its respective iteration number. The reference values, corresponding to the reconstruction with the true crystal efficiencies, are shown with cross-hairs.

We reconstructed the simulated sinograms using the proposed self-normalization algorithm. In addition, standard 3D OP-OSEM reconstructions were performed using the true crystal efficiencies to be used as the best achievable result. In the self-normalization algorithm, we evaluated the case where the gaps are previously known, as well as the case where this information is not known in advance. For each of the reconstructed images of the brain phantom, we computed the standard deviation (SD) and the mean value in the caudate and putamen. For the uniform cylinder, we computed the coefficient of variation (COV) in 9 ROIs of 30 mm diameter in each slice.

## III. Results and Discussion

In Fig. 1 the SD and mean values in the putamen are shown for the reconstructed images of the brain phantom, from the noisy sinograms with $\lambda = 10$, at each iteration of the self-normalization algorithm. These results are for the simulations using sets 1 and 4 of the crystal efficiencies and for the case where the gaps in the sinograms were included in the initial estimate of the algorithm. It is shown that the algorithm starts with larger SD (iteration 1) and converges, after iteration 2, to a similar value to that of the image reconstructed with the true crystal efficiencies. This was also observed in the values of the crystal efficiencies. The analysed images can be observed in Fig. 2. The crystal efficiencies of set 1 had a small dispersion and, for that reason, there was not a meaningful impact on the SD when not using the correct crystal efficiencies (iteration 1). Despite the significant difference between sets 1 and 4, both reconstructions achieved almost equivalent results. This result shows that the algorithm depends very little on the distribution of the crystal efficiencies.

Fig. 3 shows the reconstructed images of the noise-free sinograms for the same set of crystal efficiencies as those in Fig. 2, but in this case when not taking into account the gaps in the sinogram

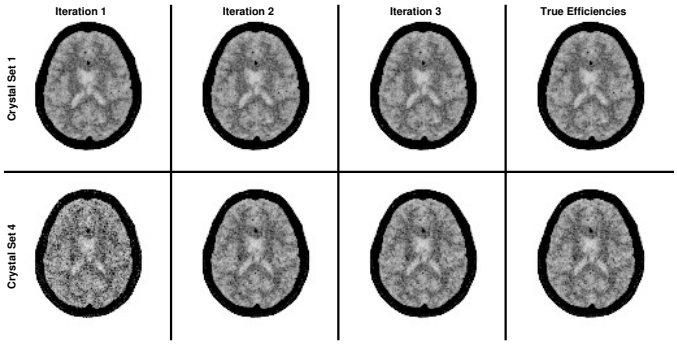


Fig. 2. Reconstructed images, as a function of iteration, for the self-normalization algorithm for sets 1 and 4 of the crystal efficiencies and using noisy sinograms ($\lambda = 10$). The sinogram gaps were included in the initial estimate of the crystal efficiencies.

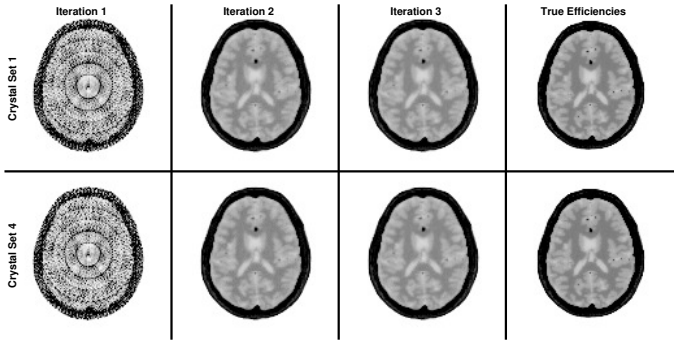


Fig. 3. Reconstructed images, as a function of iteration, for the self-normalization algorithm for sets 1 and 4 of the crystal efficiencies and using the noise-free sinograms of the brain phantom. The sinogram gaps were not included in the initial estimate of the crystal efficiencies.

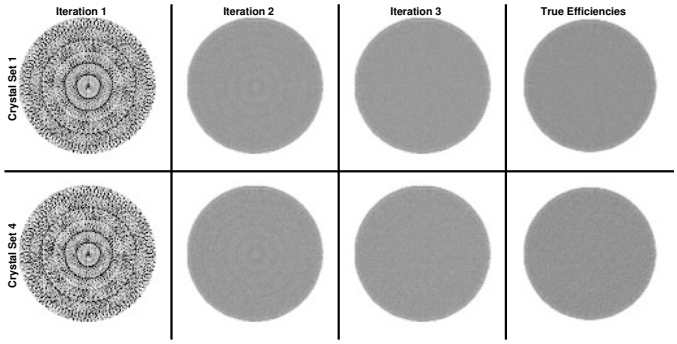


Fig. 4. Reconstructed images, as a function of iteration, for the self-normalization algorithm for sets 1 and 4 of the crystal efficiencies and using the low-noise sinograms ($\lambda = 100$) of the uniform phantom. The sinogram gaps were not included in the initial estimate of the crystal efficiencies.

in the initial estimate. It can be seen that in the first iteration, the reconstructed images have considerable artifacts due to the effect of not including the gaps in the normalization. After iteration 2 this effect is compensated. The same analysis was made with the uniform phantom (Fig. 4), where in the second iteration there are still some artifacts due to omission of the gaps in the initial estimate, but in the third iteration those artifacts are suppressed.

In Fig. 5, the COV in the ROIs of the uniform phantom are plotted for each iteration of the self-normalization algorithm, for the 4 sets of crystal efficiencies. The dashed lines mark the COV achieved

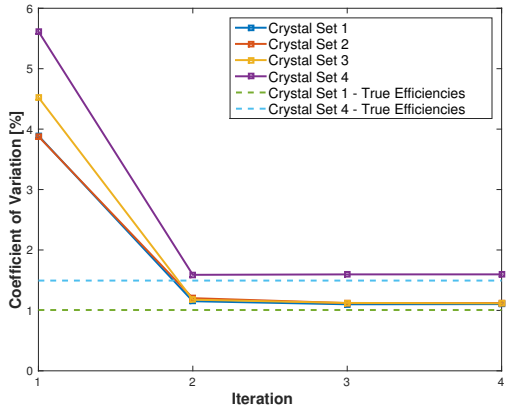


Fig. 5. COV in the ROIs of the uniform cylinder for each iteration of the self-normalization algorithm. The simulation with $\lambda = 10$ was used. Dashed lines are used to show the COV in the images reconstructed with the true crystal efficiencies.

when using the true crystal efficiencies in the reconstruction. The self-normalization algorithm achieved nearly equivalent results to using the true crystal efficiencies.

## IV. Conclusions

We presented a method to estimate scan-dependent effective crystal efficiencies. This algorithm, demonstrated on simulated data, permits the reconstruction of good quality images without having to perform a daily normalization scan, by exploiting the time-invariant NFs. The method showed good results for a variety of crystal efficiency distributions. When the gaps in the sinogram were not assumed to be known, the algorithm could estimate them but needed an additional iteration than when the gaps were included in the initial estimate.

## References

[1] R. D. Badawi and P. K. Marsden, "Developments in component-based normalization for 3D PET," Phys. Med. Biol., vol. 44, pp. 571-594, 1999.

[2] A. Ishikawa, K. Kitamura, T. Mizuta, K. Tanaka and M. Amano, "Self normalization for continuous 3D whole body emission data in 3D PET," in IEEE NSS Conf. Record, Vol. 6, pp. 3634-3637, 2004.

[3] A. Salomon et al, "A Self-Normalization Reconstruction Technique for PET Scans Using the Positron Emission Data," IEEE TMI, vol. 31, pp 2234-40, 2012.

[4] R. D. Badawi and P. K. Marsden, "Self-normalization of emission data in 3D PET," IEEE Trans Nucl Sci, vol. 46, pp. 709-712, 1999.

[5] G. Delso, S. Frst et al, "Performance Measurements of the Siemens mMR Integrated Whole-Body PET/MR Scanner," J Nucl Med, vol 52, 1914-22, 2011.

[6] M. E. Casey, H. Gadagkar, and D. Newport, "A component based method for normalization in volume PET," Proc. 3rd Int. Meeting of Fully 3D Image Reconstruction in Radiology and Nuclear Medicine, 67-71, 1995.

[7] M Defrise et al, "A normalization technique for 3D PET data," Phys. Med. Biol., vol. 36, pp. 939, 1991.

[8] R. D. Badawi et al, "Algorithms for calculating detector efficiency normalization coefficients for true coincidences in 3D PET," Phys Med Biol, vol 43, 1998.

[9] C.A. Cocosco et al, "BrainWeb: Online Interface to a 3D MRI Simulated Brain Database," NeuroImage, vol.5, no.4, part 2/4, S425, 1997 – Proc. 3rd Int. Conf. on Functional Mapping of the Human Brain, Copenhagen, May 1997.